In this study, using the method of probabilistic deterministic planning (PDP), the optimum design parameters of a standard polyethylene tank used worldwide for transporting liquid mineral fertilizers (LMF) were determined.

By the finite element method, the effect of the density of liquid mineral fertilizer, tank wall thickness and four motion modes (braking, acceleration, jump and landing) on the strength of standard polyethylene tanks was studied. According to the results of the study, the five most informative areas in the tank design were identified, for which the values of maximum stresses (σ_{max}) were obtained: filler neck, pockets, walls, tap-in points and wall transition to the tank roof. As the LMF density increases, σ_{max} in the tank increases linearly. Increasing the tank wall thickness by 1.5 times reduces the maximum stresses by 30 to 50 %. It was found that motion mode has a significant effect on the stress-strain state of a standard tank. The "heaviest" mode for a standard tank is "braking". The "acceleration" motion mode causes σ_{max} of no more than 60 % of the "braking" mode values. The "lightest" mode is "landing", in which σ_{max} is no more than 28 % relative to "braking". Based on the PDP method, equations were derived for calculating maximum stresses depending on LMF density, wall thickness and motion mode of the tank. Nomograms were built that make it possible to quickly determine the wall thickness of a standard tank without calculations, depending on external factors. The results of the study can be used in practice when designing safe and durable tanks for transporting liquid mineral fertilizers

Keywords: plastic tanks, finite element method, strength calculation, wall thickness, tank motion modes, rotational molding, rotomolding

UDC 621.22.011
DOI: 10.15587/1729-4061.2024.308904

IDENTIFICATION OF PATTERNS OF THE STRESS-STRAIN STATE OF A STANDARD PLASTIC TANK FOR LIQUID MINERAL FERTILIZERS

Vitaliy Tyukanko
Corresponding author
PhD
Department of Chemistry and Chemical Technologies**
E-mail: vetal3333@mail.ru
Alexandr Demyanenko
PhD*
Vladislav Semenyuk
Master*
Dmitriy Alyoshin
Master
Department of Sciences**
Stanislav Brilkov
Engineer***
Sergey Litvinov
Engineer***
Tatyana Shirina
Teacher**
Erlan Akhmetzhanov
Senior Lecturer, Master
Department of Arms and Shooting
Academy of the National Guard of the Republic of Kazakhstan
Zh. Kizatov str., 6, Petropavlovsk, Republic of Kazakhstan, 150000
*Department of Energetic and Radioelectronics**
**M. Kozybayev North Kazakhstan University
Pushkin str., 86, Petropavlovsk, Republic of Kazakhstan, 150000
***«AVAGRO» LLP
1st ave. Yaroslav Hasek, 8, Petropavlovsk, Republic of Kazakhstan, 150000

Received date 30.04.2024
Accepted date 10.07.2024
Published date 29.08.2024

How to Cite: *Tyukanko, V., Demyanenko, A., Semenyuk, V., Alyoshin, D., Brilkov, S., Litvinov, S., Shirina, T., Akhmetzhanov, E. (2024). Identification of patterns of the stress-strain state of a standard plastic tank for liquid mineral fertilizers. Eastern-European Journal of Enterprise Technologies, 4 (7 (130)), 47–59. https://doi.org/10.15587/1729-4061.2024.308904*

1. Introduction

Farmers in many countries around the world use liquid mineral fertilizers (LMF) to maintain high yield levels of various crops (wheat, etc.). To transport them from the storage site to a specific field (where it is planned to introduce LMF into the soil), as a rule, standard polyethylene tanks (with a volume of 2,500 to 12,000 liters) made by rotational molding are used [1–3]. However, the service life of standard polyethylene tanks, as practice has shown, is usually no more than 7 years, and then they collapse/crack due to constantly occurring dynamic loads (in the operation of the tanks).

The relevance of the scientific problem is due to the need to study the stress-strain state of polyethylene tanks for transporting liquid mineral fertilizers in order to identify areas in their design with the greatest stresses. The results of these studies are important for industry as they would allow identifying the most influencing factors on the tank strength and creating tanks with optimum design (with minimum stresses in their walls) and, accordingly, with a long service life. The destruction of polyethylene tanks for

LMF transportation is very hazardous to the environment. This is due to the fact that toxic pesticides are often added to LMF, which, when tanks are destroyed, can enter the soil and groundwater [4–6]. Thus, they harm the environment.

2. Literature review and problem statement

As shown by farmers' experience in operating mobile LMF transporters (including 4.5 m^3 tanks), the destruction of standard tanks always occurs in the same areas with maximum stresses.

Analysis of the scientific literature revealed two methods for calculating stresses in thin-walled polyethylene tanks. The first is the membrane theory of shells presented in [7–9]. The work [7] discusses various aspects of the theory of strength of materials, including the theory of shells. The paper [8] considers the differential operator of problems in the theory of membrane elastic shells and solving them using the variational-difference method, which allows analyzing and solving complex problems in the field of membrane shells. The work [9] examines geometrically nonlinear equations in the theory of membrane shells with application to problems of non-classical cylinder buckling modes, analyzing and predicting the behavior of shells under complex loads and deformations. However, this method generally does not take into account the influence of torsional and bending moments, as well as transverse forces on the stress-strain state. This is unacceptable due to the large error in the design models and the real stress-strain state of polyethylene tanks. The second is the finite element method (FEM). This method is used to calculate stress-strain states of various polymer structures experiencing hydraulic loads/pressures, mainly for pipes and tanks. In [10], FEM was successfully used to model the behavior of polyethylene pipes operating under hydraulic pressure in conditions of foundation settlement. It is shown that the strength of polyethylene pipes is significantly affected by hydraulic pressure and initial crack length. In [11], FEM was used to calculate the stress-strain state of underground polyethylene pipelines. It was found that the maximum stresses in a polyethylene pipe arise due to several factors simultaneously. As a result, factors such as soil column weight, internal hydraulic pressure, vehicle wheel load and temperature were analyzed. It is also shown that the maximum stresses in plastic pipelines are significantly influenced by the following factors: temperature, diameter of holes/defects and their specific number. However, the authors of [10, 11] did not investigate the effect of the thickness of polyethylene pipes on their stress-strain state.

In [12], the stress-strain state of two-layer plastic pipes (polyethylene and polyketone) under hydraulic pressure was studied by FEM. FEM shows that areas of maximum stresses (which are highly dependent on the pipe layer thickness) occur at the layer boundary. However, this work did not study deformations of plastic pipes. In [13], the geometric parameters of methacrylate portholes (for underwater equipment) were optimized by studying the stress-strain state. Rational porthole parameters were selected by FEM, through creating an effective stress and strain distribution, as well as improving optical characteristics. However, this work investigated the effect of hydraulic pressure on one side, and not from inside the structure. In [14], the stress-strain state of a thin-walled tank was studied by FEM and critical loads on its walls were justified. However, in this work, the thin-walled tank did not experience a uniform hydrostatic load, and forces were applied only to the upper wall section of the structure.

The FEM calculation of the stress-strain state of tanks manufactured by rotational molding began to be carried out by various groups of researchers, mainly from Southeast Asia and Europe, only over the past ten years, due to the increased speed of personal computers, which allowed complex calculations. Interesting results of FEM application are given in [15], where stress-strain states of tanks made by rotational molding from two materials: polypropylene and high-density polyethylene were studied. FEM shows that these grades of polyolefins (due to different properties) provide various deformations and stresses in tank manufacture. However, the work [15] did not study the effect of the wall thickness of tanks on their stress-strain state. In [16], stress-strain states of tanks manufactured by rotational molding were studied by FEM. Tanks are represented by two-layer structures. The effect of three types of rotational polyethylene – linear low density, linear high density and high density on the stress-strain state of two-layer tanks was investigated. FEM calculations proved that the optimum combination of the studied materials for manufacturing two-layer tanks is the use of linear low-density polyethylene for the outer layer and high-density polyethylene for the inner layer of tanks. However, the work [16] did not study the influence of geometric parameters of tanks on their stress-strain state. For underground septic tanks manufactured by rotational molding from linear polyethylene, various options for wall fabrication using foamed structures were studied using FEM [17]. Analysis of the stress-strain state of septic tanks revealed the optimum design of their walls, including the inner foamed layer of polyethylene. However, the work did not study other parameters affecting the strength of septic tanks, such as their geometric dimensions. An interesting application of FEM was proposed by the authors in [18], where, together with accelerated tests, the long-term strength parameters of products made by rotational molding from two materials – linear polyethylene and polypropylene were analyzed. However, this work did not take into account the effect of dynamic loads possible during the operation of products on the long-term strength.

Summarizing the above studies, we can conclude that for plastic structures (pipes, tanks, etc.) experiencing various dynamic loads, the stress-strain state depending on the main influencing parameters was not studied:

– wall thickness – was not considered in [10, 11, 15];

– hydrostatic pressure direction – was not considered in [13];

– load application uniformity – was not considered in [14];

– geometric parameters (stiffeners and other elements) [15–17];

– various dynamic loads – were not considered in [10–18].

In addition, deformations of structures depending on their stress-strain state were not studied – they were not considered in [12, 16].

3. The aim and objectives of the study

The aim of the study is to identify patterns in the stress-strain state of a standard polyethylene tank used for transporting liquid mineral fertilizers. This will make it possible to create tanks with optimum design (with minimum stresses in their walls) and, accordingly, with a long service life (at least 25 years).

To achieve the aim, the following objectives were set:

– using the finite element method, to investigate the effects of liquid mineral fertilizer density, wall thickness and motion modes on stresses in fixed areas of a standard tank;

– using the method of probabilistic deterministic planning, to construct nomograms and approximation equations that take into account the effects of liquid density and wall thickness on maximum stresses.

4. Materials and methods

4. 1. Object and hypothesis of the study

The object of the study is a standard 4.5 m^3 storage tank for LMF (Fig. 1).

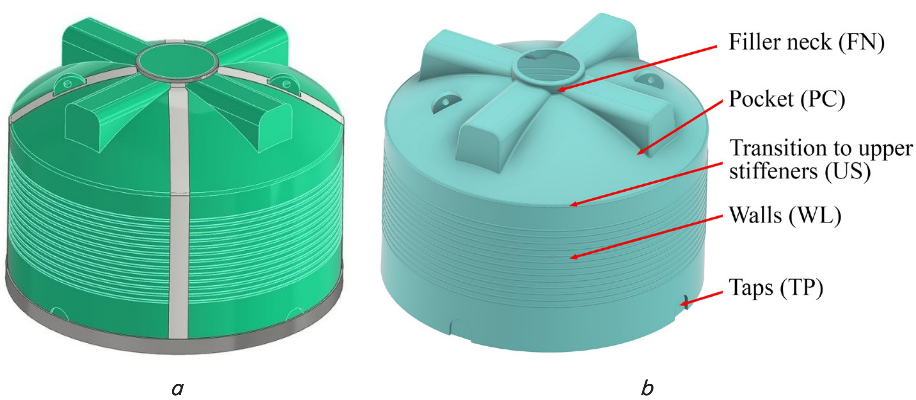

Fig. 1. 3D model of a 4.5 m^3 tank: *a* — with fasteners (in the bed); *b* — fixed areas for FEM stress calculations

The tank material is high-density polyethylene (HDPE) Lupolen 4021 KRM with the following mechanical properties: density – 939.5 kg/m^3, elastic modulus – 750 MPa, Poisson's ratio – 0.45, a standard value for this class of polymers was taken. The tank diameter is 2,200 mm, height is 1,590 mm.

The hypothesis of the study: calculations by the FEM method together with the PDP method allow optimizing the design of a standard polyethylene tank for LMF transportation.

4. 2. Experimental design

As shown by farmers' experience in operating standard tanks (for transporting liquid mineral fertilizers), their service life can be significantly influenced by several different factors: the density of the transported LMF, operating conditions (transportation speed and field unevenness) and various geometric parameters of the barrel (wall thickness, etc.). To account for the combined effect of these parameters on the stress-strain state of a standard polyethylene tank, in this paper we use the method of probabilistic deterministic planning (PDP) [19]. It allows us to derive mathematical multifactor relationships describing the effect of the above parameters on maximum stresses in the tank. The methodology of probabilistic deterministic planning is given in detail in [19–23].

The expediency of using the PDP method (and as a result, deriving equations/nomograms) to calculate the stress-strain state of standard plastic tanks is explained by the lack of specialists capable of performing FEM calculations in the vast majority of companies engaged in rotational molding.

The experiment was designed in accordance with the probabilistic deterministic planning (PDP) method [19]. The effect of such parameters as liquid mineral fertilizer density, wall thickness and motion modes ("braking", "acceleration", "landing" and "jump") on stresses in the most loaded areas of a standard polyethylene tank for transporting liquid mineral fertilizers was studied.

For each of the motion modes, a 3×3 experimental design was developed. Two parameters were varied on three levels:

– the density of liquid mineral fertilizer (p, kg/m^3) took the values: 1,000, 1,300 and 1,700;

– the wall thickness (L, mm) took the values: 8, 10 and 12.

Tables 1–4 present experimental designs for four motion modes with the maximum stress (σ_{max}, MPa) in the most loaded areas of the tank.

Table 1

Effect of p and L on σ_{max}, under "braking" mode conditions

No.	L, mm	p, kg/m^3	Maximum stresses in the studied tank areas, MPa				
			WL	PC	FN	TP	US
1	8	1,000	8.58	41.59	21.01	5.70	33.30
2	10	1,000	6.80	29.37	16.70	4.30	24.90
3	12	1,000	5.60	22.10	12.13	3.47	17.81
4	8	1,300	11.23	54.81	25.50	7.41	43.57
5	10	1,300	8.88	38.69	20.06	5.67	33.39
6	12	1,300	7.30	29.11	16.00	4.49	26.18
7	8	1,700	14.37	70.50	32.77	9.64	57.53
8	10	1,700	11.35	49.75	25.82	7.32	43.04
9	12	1,700	9.32	37.44	20.60	5.76	33.73

Table 2

Effect of p and L on σ_{max}, under "acceleration" mode conditions

No.	L, mm	p, kg/m^3	Maximum stresses in the studied tank areas, MPa				
			WL	PC	FN	TP	US
1	8	1,000	5.29	20.51	11.07	2.81	16.50
2	10	1,000	4.24	14.58	7.40	1.05	12.45
3	12	1,000	3.55	10.98	5.80	0.70	9.78
4	8	1,300	6.93	27.02	12.86	3.20	22.07
5	10	1,300	5.55	19.21	9.83	2.75	16.52
6	12	1,300	4.64	14.47	8.10	2.22	12.95
7	8	1,700	8.88	34.76	16.56	4.77	28.45
8	10	1,700	7.11	24.72	12.66	3.54	21.28
9	12	1,700	5.93	18.62	10.43	2.88	16.70

Table 3

Effect of p and L on σ_{max}, under "jump" mode conditions

No.	L, mm	p, kg/m^3	Maximum stresses in the studied tank areas, MPa				
			WL	PC	FN	TP	US
1	8	1,000	3.36	5.00	2.59	3.10	3.60
2	10	1,000	2.83	3.63	1.52	2.30	2.60
3	12	1,000	2.46	2.74	1.26	1.90	2.00
4	8	1,300	4.39	6.62	2.71	3.99	4.83
5	10	1,300	3.70	4.80	2.10	2.99	3.52
6	12	1,300	3.20	3.64	1.68	2.45	2.74
7	8	1,700	5.62	8.54	3.51	5.18	6.27
8	10	1,700	4.73	6.20	2.73	4.38	4.61
9	12	1,700	4.09	4.70	2.19	3.17	3.60

Table 4

Effect of p and L on σ_{max}, under "landing" mode conditions

No.	L, mm	p, kg/m^3	Maximum stresses in the studied tank areas, MPa				
			WL	PC	FN	TP	US
1	8	1,000	2.39	12.20	10.75	0.87	14.83
2	10	1,000	2.00	9.11	7.68	0.80	11.10
3	12	1,000	1.77	7.29	6.19	0.70	8.71
4	8	1,300	3.14	17.05	11.69	1.14	19.52
5	10	1,300	2.65	12.60	10.13	1.05	14.60
6	12	1,300	2.31	9.21	8.16	0.95	11.46
7	8	1,700	4.03	20.70	16.33	1.47	25.10
8	10	1,700	3.40	15.45	13.03	1.34	18.77
9	12	1,700	2.96	11.85	10.49	1.18	14.72

Design loads of various motion modes ("braking", "acceleration", "landing" and "jump") are given in section 4. 3. 4.

4. 3. Method of calculating the strength properties of a 4.5 m^3 tank

4. 3. 1. Calculation steps

The method of calculating the strength properties of the tank includes the following seven steps:

– importing the model geometry to Parasolid and adjusting the tank geometry;

– creating all materials used in the calculation indicating their physicomechanical properties (density, elastic modulus, yield strength, Poisson's ratio);

– building a finite element grid based on the edited geometry;

– specifying loads (hydrostatic pressure and tank dead weight) and directions of their impact;

– fasteners and contacts;

– Simcenter Nastran solver settings;

– carrying out calculations.

There is a wide variety of elements in the Femap software package, for example: Rod element, Tube element, Bar element, Beam element, Spring element, Shear Panel element, Membrane element, Bending Only element, Plate element, Plot Only element, volumetric, Solid element and others. The result of the FEM calculation depends on the correct choice of the element type. For solid bodies composed of several thin elements with a constant or piecewise linear thickness, finite elements based on midsurfaces are used. Such bodies include shell mold bodies, containers, tanks, cisterns, sheet parts of assembly units. That is why the method of midsurface creation was chosen to calculate the 4.5 m^3 tank, and the Plate type element was chosen as a shell element.

The location of an element in space is described by the coordinates of the nodes belonging to the object. Each element node is characterized by nodal displacements. The first three nodal displacements mean movements along the coordinate axes, the second three degrees of freedom mean rotations around the vectors that define these directions. The list of the model degrees of freedom is determined by the type of elements used in the simulation. All six displacement components are defined in nodes of shell elements in bending and torsion.

In this study, all six degrees of freedom are constrained for the steel bed on which the tank rests with its lower part. A "Contact" type interface is set between the tank and the steel strips, with a coefficient of polyethylene friction over steel. When performing a numerical analysis in Femap, a series of calculations were made for a 4.5 m^3 tank in order to determine the optimum size of the finite element grid. By analyzing the data obtained, the value of 15 mm was selected for further calculations (Fig. 2). This is due to the fact that with a decrease in this parameter, the calculation time increased many times, and the stresses increased slightly. For example, for a 10 mm finite element grid (Fig. 3), the calculation time increased by 2 times, and the stresses at critical points increased by only 3.3 %.

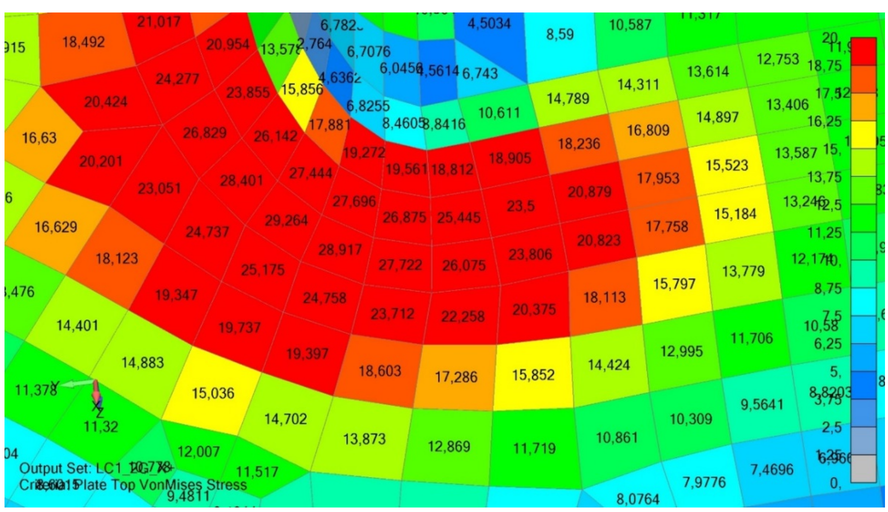

Fig. 2. Finite element model with a grid size of 15 mm

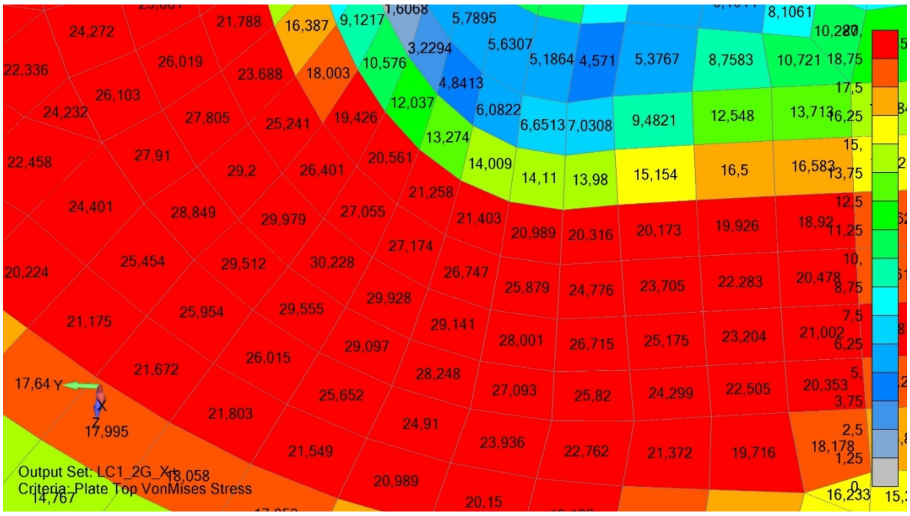

Fig. 3. Finite element model with a grid size of 10 mm

4. 3. 2. Importing the model geometry to Parasolid and adjusting the tank geometry

The model for developing the calculation methodology is a 4.5 m^3 tank for storing and transporting liquid mineral fertilizers. A general view of the tank is shown in Fig. 4.

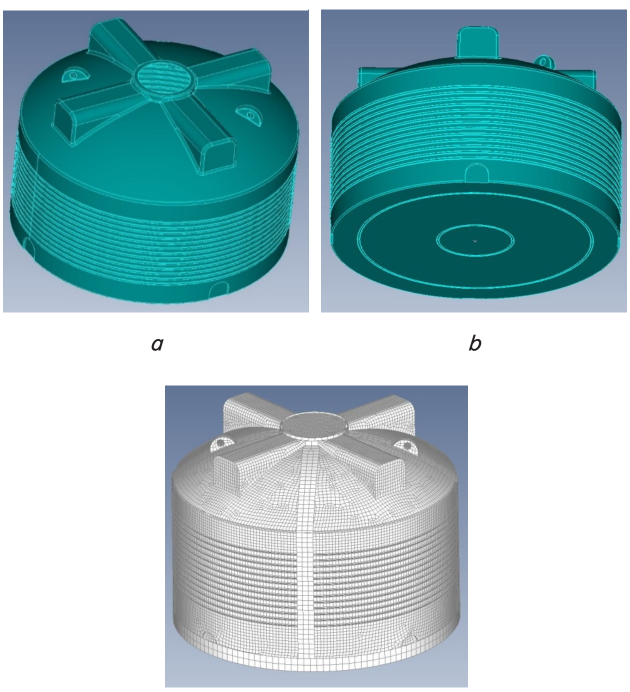

a *b*

c

Fig. 4. General view of a standard 4.5 m^3 polyethylene storage tank for LMF: *a* – isometry of the upper part; *b* – isometry of the lower part; *c* – finite element model constructed

The program allows you to configure material properties, build a finite element grid, and specify required loads.

4. 3. 3. Building a finite element grid

Based on the created midsurfaces, it is now necessary to build a shell finite element grid. Element type – PSHELL, three- and four-node shell linear elements. The total number of finite elements is 40,229. The number of nodes is 40,595. The finite element model is shown in Fig. 4, *c*.

4. 3. 4. Specifying loads

According to E-ECE-TRANS-505 [24], the FEM calculation was carried out for four operating modes of a standard tank: "Braking" mode – the action of double the mass of the tank and LMF – in the direction of motion; the acting loads – double the mass of the tank (F_1) and LMF (F_2) – in the direction of motion are shown in Fig. 5.

"Acceleration" mode – the action of a single mass of the tank and LMF – in the opposite direction relative to vehicle motion; the acting loads – the mass of the tank (F_1) and LMF (F_2) are shown in Fig. 6.

"Landing" mode – the action of double the mass of the tank and LMF – in the positive direction of gravity; the acting loads – double the mass of the tank (F_1) and LMF (F_2) – in the vertical direction from top to bottom are shown in Fig. 7.

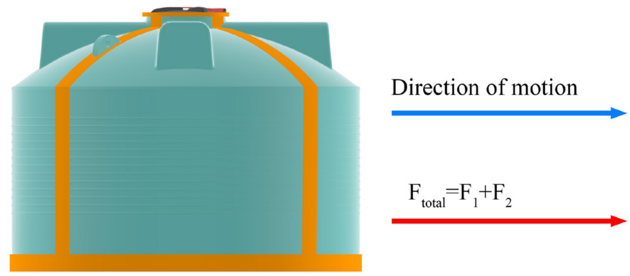

Fig. 5. Action of double the mass of the tank and liquid mineral fertilizers in the direction of motion

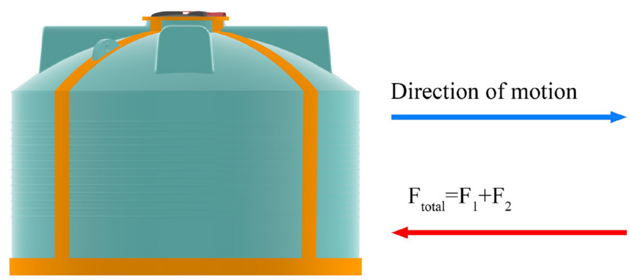

Fig. 6. Action of a single mass of the tank and liquid mineral fertilizers in the opposite direction relative to motion

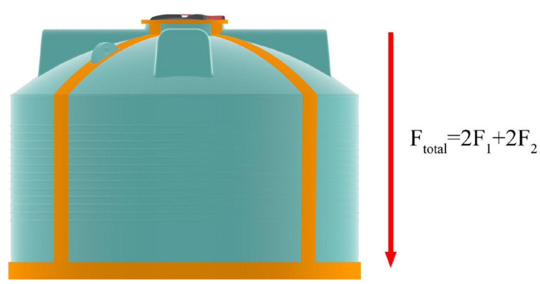

Fig. 7. Action of double the mass of the tank (F_1) and liquid mineral fertilizers (F_2) – in the vertical direction from top to bottom

"Jump" mode – the action of a single mass of the tank and LMF – in the opposite direction relative to gravity; the acting loads – the total mass of the tank (F_1) and LMF (F_2) – in the vertical direction from bottom to top are shown in Fig. 8.

To account for the tank dead weight, accelerations are applied to the model in the appropriate directions. The acceleration amplitude is 9.81 m/s^2.

The action of the liquid mass was modeled by hydrostatic pressure varying in directions corresponding to the load directions. The hydrostatic pressure amplitude is determined by the formula (1):

$$P=\rho \cdot g \cdot h, \quad (1)$$

where ρ=1,000, 1,300 or 1,700 kg/m^3 – liquid density;

g=9.81 mm/s^2 – acceleration of gravity;

h – head, m.

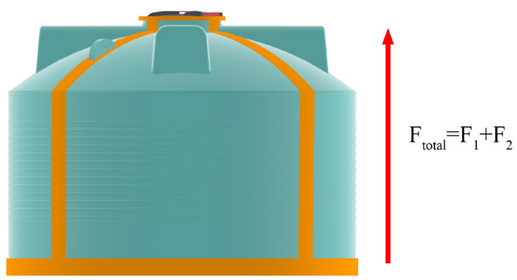

Fig. 8. Action of the total mass of the tank (F_1) and LMF (F_2) – in the vertical direction from bottom to top

4. 3. 5. Fasteners and contacts

The bottom of the tank rests on a steel bed. At the top, the tank is fixed with a steel ring at the filler neck, and a steel strip on the sides. The contact surfaces are given a friction coefficient of 0.1.

4. 3. 6. Solver settings

The calculation was performed in the SOL 101 linear static solver. This solver uses the following assumptions – the linear behavior of the material and the hypothesis of small displacements (the effects of geometric nonlinearity are not taken into account). The only source of nonlinearity is contact nonlinearity.

5. Results of the stress-strain state study of a standard plastic tank

5. 1. Results of the tank strength calculation by the finite element method

5. 1. 1. Results of calculating maximum stresses in the "Braking" mode

The result of calculating the polyethylene tank in the "braking" mode is shown in Fig. 9 (for a wall thickness of 10 mm and transported LMF density of 1,000 kg/m^3).

The effect of tank wall thickness on maximum stresses is shown in Fig. 10, *a–c*, respectively.

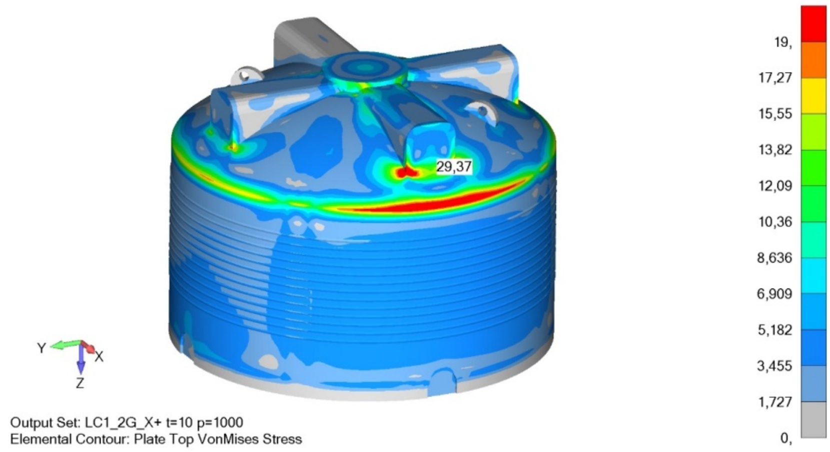

Fig. 9. Result of the FEM calculation of a standard 4.5 m^3 barrel under conditions of the "braking" mode, wall thickness of 10 mm, LMF density of 1,000 kg/m^3

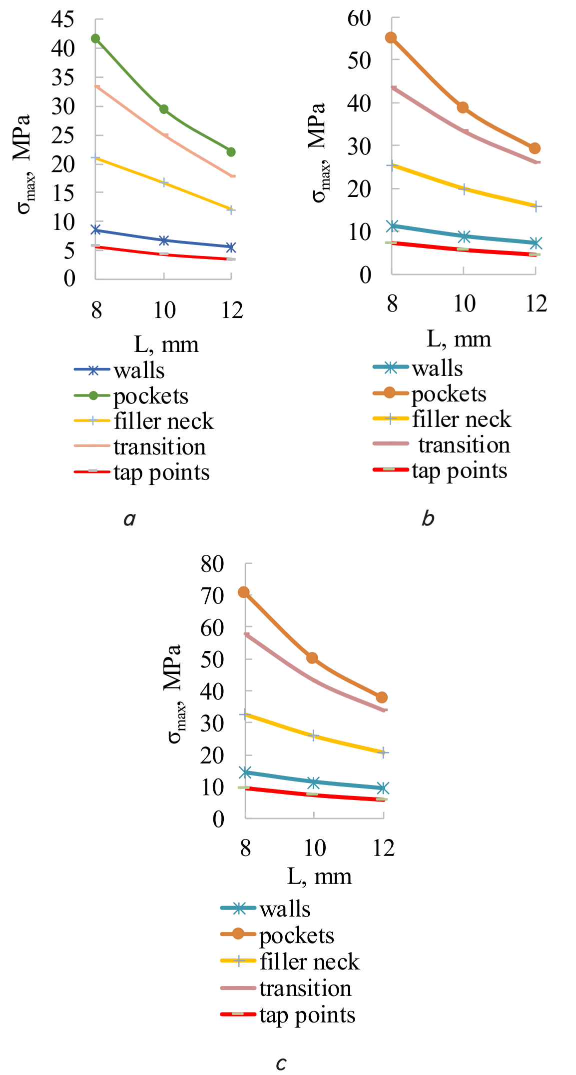

Fig. 10. Effect of wall thickness on maximum stresses in the five studied tank sections characteristic of the "braking" mode at different transported liquid densities: *a* – 1,000 kg/m^3; *b* – 1,300 kg/m^3; *c* – 1,700 kg/m^3

The effect of LMF density on maximum stresses is shown in Fig. 11, *a–c*, respectively.

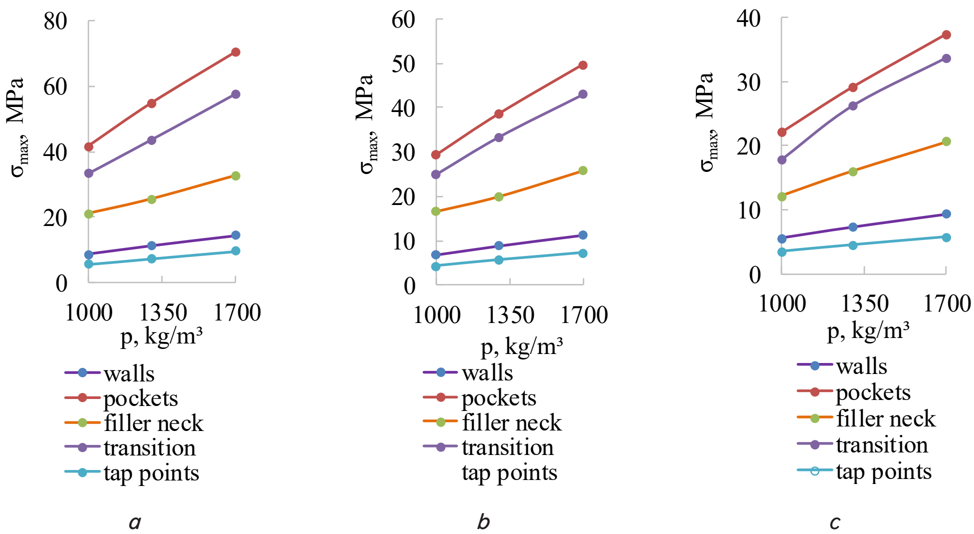

Fig. 11. Effect of transported liquid density on maximum stresses in the five studied tank sections characteristic of the "braking" mode at different wall thicknesses: *a* – 8 mm; *b* – 10 mm; *c* – 12 mm

According to Fig. 10, 11, it is possible to correlate different maximum stresses occuring in a standard tank in the "braking" motion mode.

stresses occuring in a standard tank in the "acceleration" motion mode.

5. 1. 2. Results of calculating maximum stresses in the "Acceleration" mode

The result of calculating the polyethylene tank in the "acceleration" mode is shown in Fig. 12 (for a wall thickness of 10 mm and transported LMF density of 1,000 kg/m^3).

The effect of tank wall thickness on maximum stresses is shown in Fig. 13, *a–c*, respectively.

The effect of the density of transported liquid mineral fertilizer on maximum stresses is shown in Fig. 14, *a–c*, respectively.

According to Fig. 13, 14, it is possible to correlate different maximum

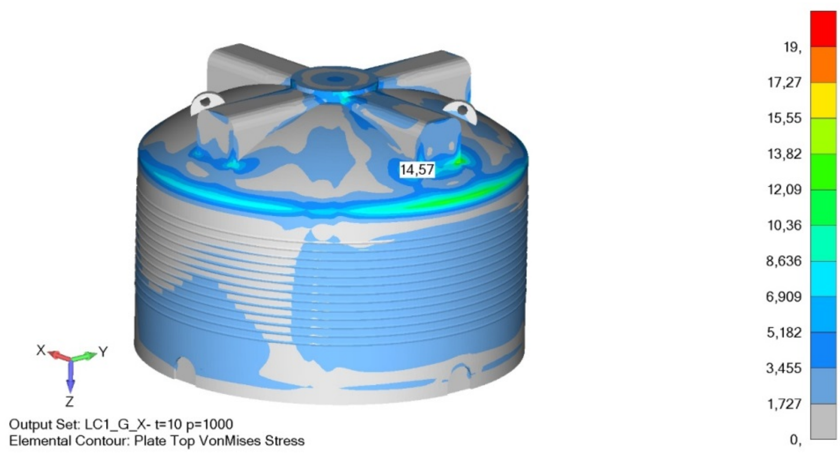

Fig. 12. Result of the FEM calculation of a standard 4.5 m^3 barrel under the conditions of the "acceleration" mode, wall thickness of 10 mm, LMF density of 1,000 kg/m^3

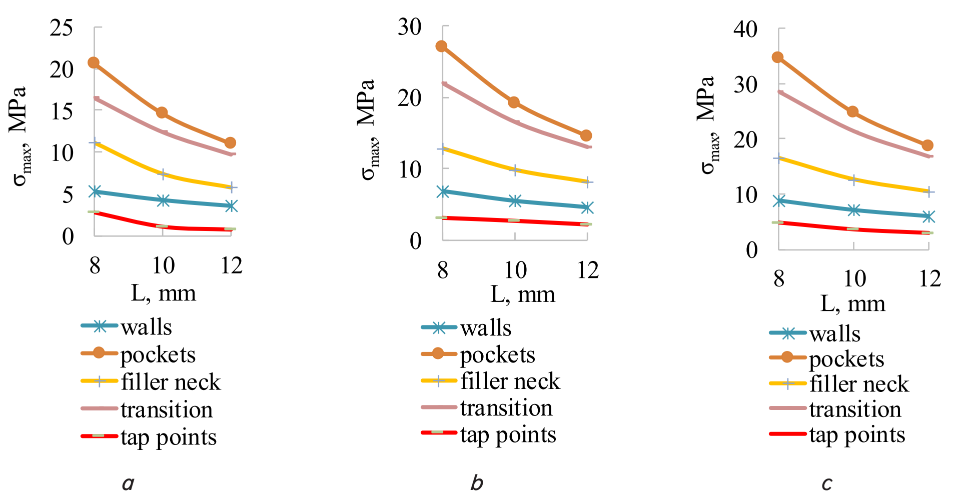

Fig. 13. Effect of wall thickness on maximum stresses in the five studied tank sections characteristic of the "acceleration" mode at different transported liquid densities: *a* – 1,000 kg/m^3; *b* – 1,300 kg/m^3; *c* – 1,700 kg/m^3

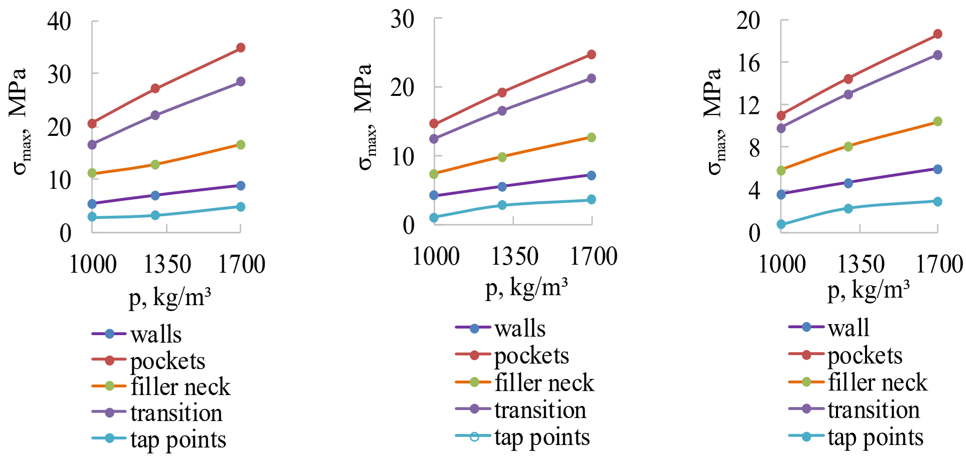

a *b* *c*

Fig. 14. Effect of transported liquid density on maximum stresses in the five studied tank sections characteristic of the "acceleration" mode at different wall thicknesses: *a* – 8 mm; *b* – 10 mm; *c* – 12 mm

5. 1. 3. Results of calculating maximum stresses in the "Landing" mode

The result of calculating the polyethylene tank in the "landing" mode is shown in Fig. 15 (for a wall thickness of 10 mm and transported LMF density of 1,000 kg/m^3).

Graphs of the effect of tank wall thickness on maximum stresses are shown in Fig. 16, *a–c*, respectively.

The effect of LMF density on maximum stresses is shown in Fig. 17, *a–c*.

According to Fig. 16, 17, it is possible to correlate different maximum stresses occuring in a standard tank in the "landing" motion mode.

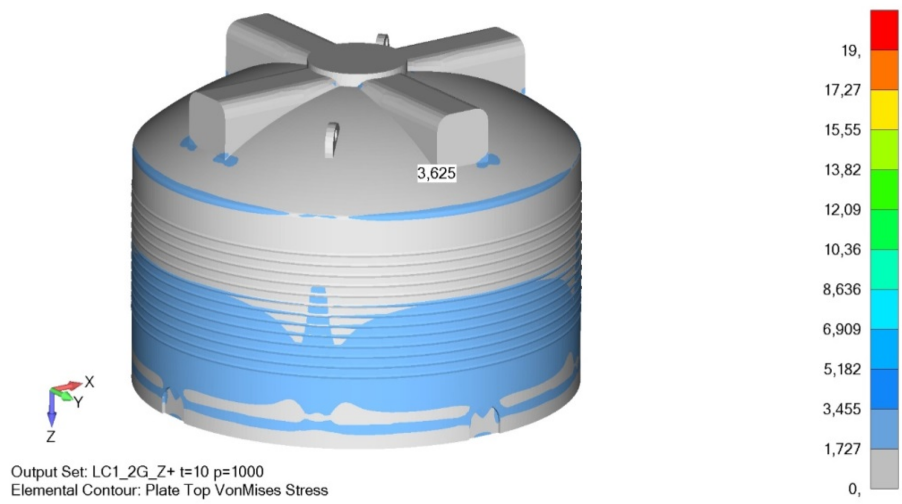

Fig. 15. Result of the FEM calculation of a standard 4.5 m^3 barrel in the conditions of the "landing" mode, wall thickness of 10 mm, LMF density of 1,000 kg/m^3

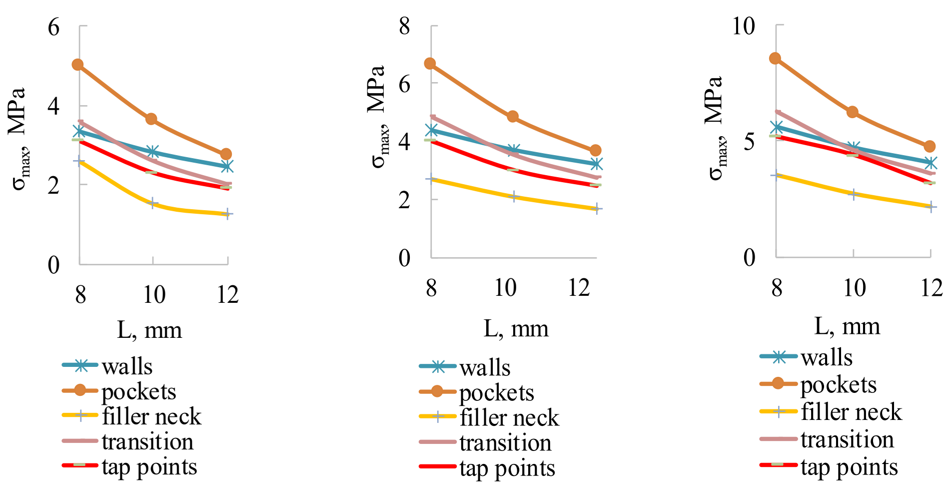

a *b* *c*

Fig. 16. Effect of wall thickness on maximum stresses in the five studied tank sections characteristic of the "landing" mode at different transported liquid densities: *a* – 1,000 kg/m^3; *b* – 1,300 kg/m^3; *c* – 1,700 kg/m^3

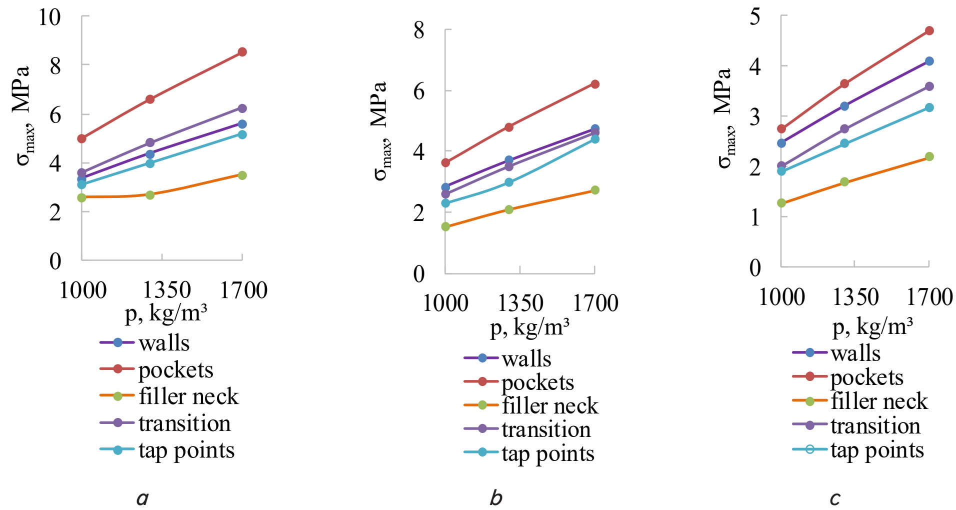

Fig. 17. Effect of transported liquid density on maximum stresses in the five studied tank sections characteristic of the "landing" mode at different wall thicknesses: *a* – 8 mm; *b* – 10 mm; *c* – 12 mm

5. 4. 1. Results of calculating maximum stresses in the "Jump" mode

The result of calculating the polyethylene tank in the "jump" mode is shown in Fig. 18 (for a wall thickness of 10 mm and transported LMF density of 1,000 kg/m^3).

The effect of tank wall thickness on maximum stresses is shown in Fig. 19, *a–c*, respectively.

Graphs of the effect of transported liquid density on maximum stresses in the five studied sections at different wall thicknesses of 8 mm, 10 mm, 12 mm are shown in Fig. 20, *a–c*, respectively.

According to Fig. 19, 20, it is possible to correlate different maximum stresses occuring in a standard tank in the "jump" motion mode.

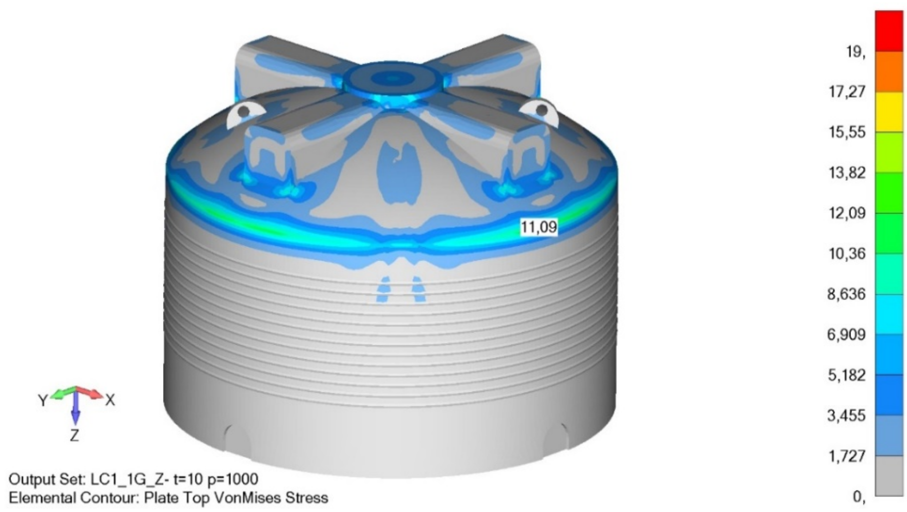

Fig. 18. Result of the FEM calculation of a standard 4.5 m^3 barrel under the conditions of the "jump" mode, wall thickness of 10 mm, LMF density of 1,000 kg/m^3

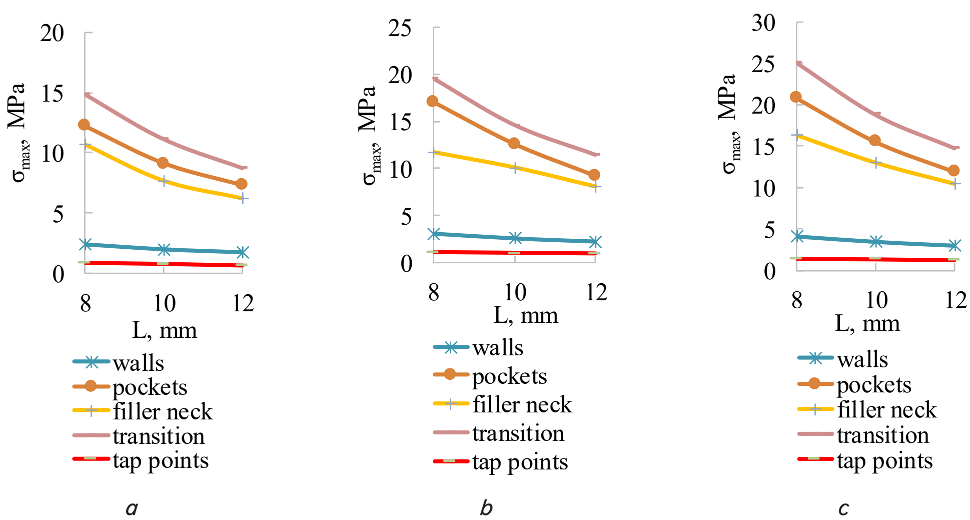

Fig. 19. Effect of wall thickness on maximum stresses in the five studied tank sections characteristic of the "jump" mode at different transported liquid densities: *a* – 1,000 kg/m^3; *b* – 1,300 kg/m^3; *c* – 1,700 kg/m^3

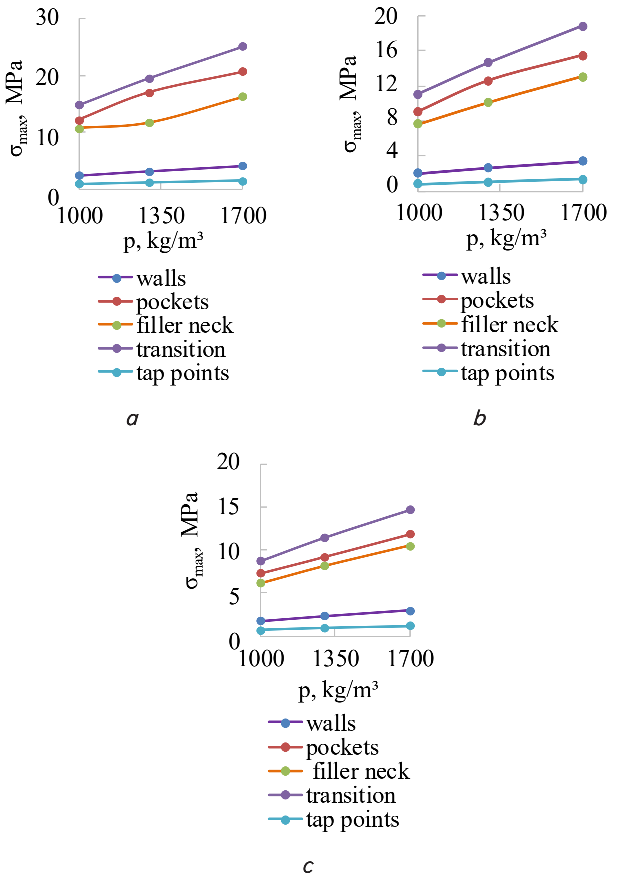

Fig. 20. Effect of transported liquid density on maximum stresses in the five studied tank sections characteristic of the "jump" mode at different wall thicknesses: *a* – 8 mm; *b* – 10 mm; *c* – 12 mm

5. 2. Results of modeling the effect of liquid density and wall thickness on maximum stresses

According to the method of probabilistic deterministic planning [19–23], for each of the motion modes, two-parameter mathematical models based on the generalized equation (2) were constructed:

$$\sigma_{max} = \frac{(a+b\cdot L)\cdot(c+d\cdot p)}{\sigma_{av}}, \text{ MPa}, \quad (2)$$

where *a*, *b*, *c* and *d* are the coefficients of partial dependencies;

σ_{av} is the general average of the maximum stress, MPa.

The general average of the maximum stress (σ_{av}, MPa) is an arithmetic mean of all experimental values of the maximum stresses for each specific studied tank area and motion mode, presented in Tables 1–4.

The values of the coefficients *a*, *b*, *c* and *d*, as well as the general average of the maximum stress (σ_{av}, MPa) for each studied tank area for each motion mode are presented in Table 5.

The adequacy of the obtained mathematical model was estimated using the nonlinear multiple correlation coefficient – its value for the presented models is not less than 0.75.

To quantify the effect of wall thickness on σ_{max} in the tank, we use the stress reduction factor (SRF), which is found by the following formula (3):

$$SRF = \frac{\sigma_8 - \sigma_{12}}{\sigma_8} 100\,\%, \quad (3)$$

where σ_8 is the maximum stress in the tank with a thickness of 8 mm, σ_{12} is the maximum stress in the tank with a thickness of 12 mm.

Fig. 21, *a*, *b* show diagrams of changes in SRF in five studied sections of a standard barrel with an increase in wall thickness by 50 % (from 8 to 12 mm), under conditions of different transported liquid densities (1,000 and 1,700 kg/m^3) and four tank motion modes.

Table 5

Values of the coefficients, as well as the general average of the maximum stress for each studied tank area in four motion modes

No.	Tank motion modes	Studied tank area	Values of the coefficients and the general average of the maximum stress				
			A	*b*	*c*	*d*	σ_{av}
1	Braking	WL	19.327	–0.9967	0.3673	0.0067	9.27
2		PC	106.69	–6.5208	0.5607	0.0307	41.48
3		FN	46.635	–2.5458	2.4902	0.014	21.18
4		TP	13.498	–0.7525	0.1085	0.0044	5.97
5		US	82.061	–4.7233	–2.0527	0.0277	34.83
6	Acceleration	WL	11.608	–0.5817	0.1935	0.0042	5.79
7		PC	52.391	–3.185	0.2588	0.0152	20.54
8		FN	23.99	–1.3467	0.754	0.0073	10.52
9		TP	6.8078	–0.415	–1.5056	0.0031	2.66
10		US	40.403	–2.2992	–0.1198	0.0131	17.41
11	Jump	WL	6.8367	–0.3017	0.1533	0.0028	3.82
12		PC	12.663	–0.7567	–0.0132	0.0038	5.10
13		FN	5.3211	–0.3067	0.3001	0.0015	2.25
14		TP	7.2317	–0.3958	–0.1861	0.0026	3.27
15		US	9.0522	–0.53	–0.2232	0.003	3.75
16	Landing	WL	4.8389	–0.21	0.0608	0.002	2.74
17		PC	30.829	–1.8	0.6283	0.0092	12.83
18		FN	22.103	–1.1608	0.7545	0.0073	10.49
19		TP	1.5972	–0.0542	0.0315	0.0008	1.06
20		US	35.89	–2.0467	0.2576	0.0114	15.42

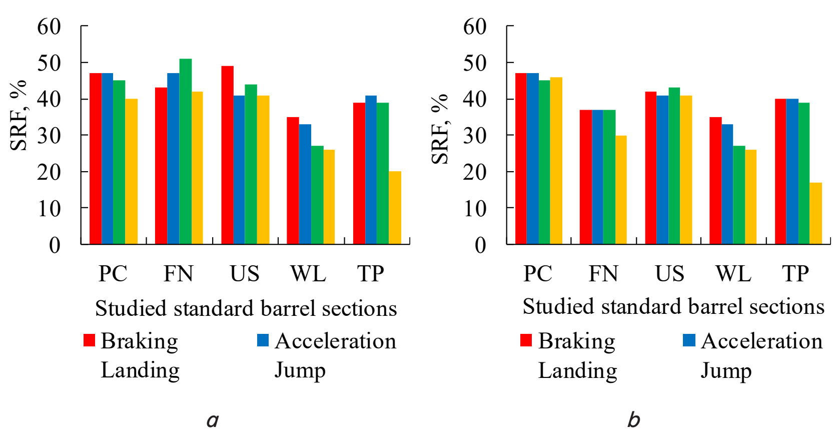

Fig. 21. Effect of tank motion modes on changes in the stress reduction factor (SRF) with an increase in wall thickness from 8 to 12 mm (at a transported liquid density: *a* – 1,000 kg/m^3; *b* – 1,700 kg/m^3)

To find the maximum stresses in the tank, nomograms were constructed (Fig. 22).

The results of FEM calculations are consistent with the tests of a standard barrel carried out at the AVAGRO LLP production enterprise (Fig. 23).

Destruction of a 4.5 m^3 tank during field tests occurs in stress concentrator areas. Maximum stresses in these tank areas were revealed by FEM calculations.

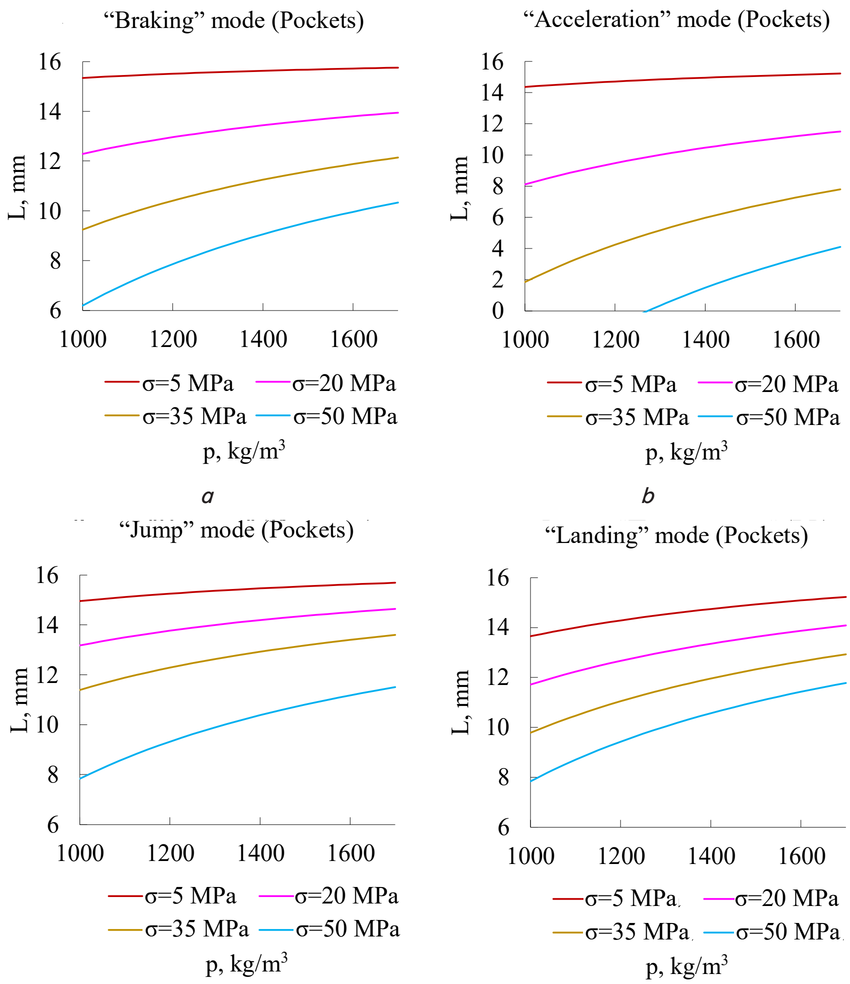

Fig. 22. Nomograms $L=f(p, \sigma_{max})$ for finding the wall thickness for different densities of transported liquid fertilizers and the specified maximum stress in the most loaded tank section: *a* – “Braking” mode; *b* – “Acceleration” mode; *c* – “Jump” mode; *d* – “Landing” mode

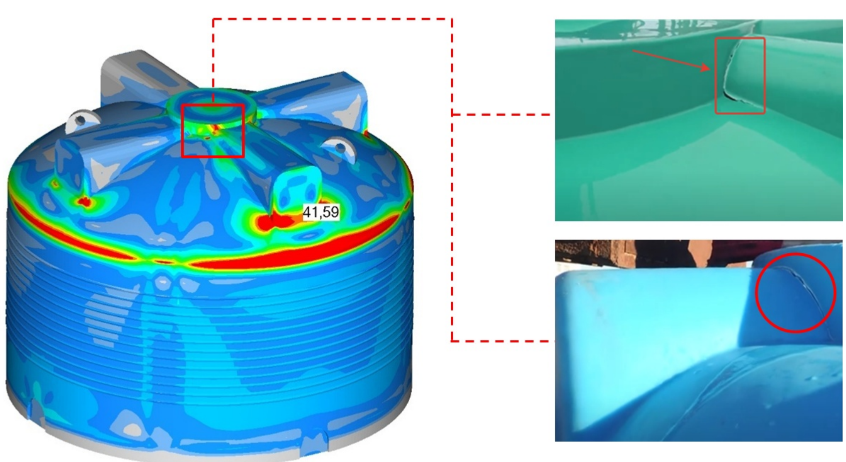

Fig. 23. Fragments of tank tests at AVAGRO LLP indicating cracks that occurred in the filler neck area (FN)

6. Discussion of the results of the stress-strain state study of a standard plastic tank

Of the four studied motion modes for a standard barrel, “braking” is the most loaded in terms of maximum stresses, followed by “acceleration”, “jump” and the last is “landing” (Fig. 9–20). At the same time, depending on the influencing factors, the maximum stresses (relative to those characteristic of the “braking” mode) can be expressed as a percentage: “braking” – 100 %, “acceleration” – 44–58 %, “jump” – 30–43 % and “landing” – 10–28 % (Fig. 9–20 and Tables 1–4).

The destruction areas revealed during field tests of standard tanks (water-filled tanks were dropped from a height of 1.5...2 meters) coincided with areas of maximum stresses, according to FEM calculations (Fig. 23). The maximum values of the parameter σ_{max} are characteristic of the following combination of the influencing factors: the “braking” mode, the minimum wall thickness (8 mm) and the maximum transported fertilizer density (1,700 kg/m^3) (Fig. 10, *c*, 11, *a*). At the same time, σ_{max} in the PC region is 70.5 MPa, for US 57.53MPa and FN – 32.77 MPa (Fig. 10, *c*, 11, *a*). Under similar conditions, with an increase in the tank wall thickness (from 8 to 12 mm), the maximum stresses in the PC region are already 37.44 MPa, in the US region 33.73 MPa and FN – 20.60 MPa (Fig. 10, *c*, 11, *c*). Thus, an increase in the tank wall thickness by 50 % (from 8 to 12 mm) can significantly reduce the maximum stresses (Fig. 9–20 and Tables 1–4). Estimating the influence of the tank motion modes on SRF (Fig. 21, *a*, *b*), it can be noted that the “jump” mode is least susceptible to an increase in wall thickness. And the modes with the maximum revealed SRF, depending on the studied tank areas, are: “braking”, “landing” and “acceleration” (Fig. 9–20 and Tables 1–4).

Therefore, it can be concluded that the strength of a plastic tank made by rotational molding is largely determined by the wall thickness (Fig. 10, 13, 16, 19). This correlates with the works [14, 17], showing that in order to ensure the long-term stability of a polyethylene tank, it is necessary to guarantee the necessary bending stiffness of the walls. The guaranteed bending stiffness of the tank walls can be achieved through the wall thickness or using foam structures. Besides, high-strength materials, in particular polypropylene, can be used for this purpose [16]. According to SRF (Fig. 21), the five studied sections of a standard tank, according to the degree of susceptibility to plastic thickness increase, can be arranged in a row (in decreasing order): FN>PC>US>TP>WL. For FN, SRF is 51 %, and for WL, SRF does not exceed 35 % (Fig. 21). Therefore, we can conclude that it is expedient to increase the wall thickness for the most loaded areas in the tank structure (FN, PC and US) (Fig. 21). Increasing the wall thickness in the WL region is not advisable, due to a small decrease in σ_{max} with a significant increase in plastic consumption and, consequently, the cost of the tank.

The density of the transported liquid mineral fertilizer largely determines stresses in a standard barrel (Fig. 11, 14, 17, 20); so, an increase in LMF density from 1,000 to 1,700 kg/cm^3 increases σ_{max} by an average of 1.85 times. There is a linear relationship $\sigma_{max}=f(\text{p})$, as shown in Fig. 11, 14, 17, 20. Of all the studied modes, "jump" is the most sensitive to changes in LMF density (Fig. 11, 14, 17, 20). At the same time, tank destruction when transporting LMF with maximum density is possible in the following areas: filler neck (FN) or pockets (PC) (Fig. 23).

In this study, using the PDP method, approximation equations (two-factor statistical mathematical models) were obtained that take into account the effect of the wall thickness and LMF density (2) on the maximum stresses (in the five studied areas) of a standard tank. These models can be used to determine the optimum tank wall thickness, providing minimum stresses and, accordingly, maximum service life. Using nomograms (Fig. 22, *a–d*), it is possible to visually assess the effect of wall thickness and density on the maximum stresses in the design of a standard tank.

The results of this study can only be used to determine the wall thickness of standard tanks with a transported LMF density not exceeding 1,700 kg/m^3. When transporting LMF with a density of 1,750 kg/m^3 or more, equation (2) and the nomograms in Fig. 22 are not applicable.

Model designs with different radii of the tank roof transition to the upper stiffeners were not studied. Therefore, a logical continuation of this study to reduce stresses and increase the service life is to change the design of a standard tank adjusting the filler neck geometry and increasing the radius of the tank roof transition to the upper stiffeners.

7. Conclusions

1. With an increase in the density of the transported liquid mineral fertilizer (LMF), the maximum stresses in a standard barrel increase linearly. An increase in LMF density from 1,000 to 1,700 kg/cm^3 leads to an increase in σ_{max} by an average of 1.85 times. The most sensitive to changes in LMF density is the "jump" motion mode of the tank. Increasing the tank wall thickness by 1.5 times (from 8 to 12 mm) can reduce maximum stresses by 30 to 50 %, depending on the motion mode. The stress-strain state study of a standard tank in five different areas/sections revealed that the most susceptible areas to plastic thickness increase are the filler neck (FN and pockets (PC) areas, and the least – tank walls (WL). Therefore, to minimize stress in the filler neck and pocket areas, we recommend increasing the plastic thickness. However, an increase in the tank wall thickness may not be economically justified, due to a small decrease in stresses with a significant increase in the cost of the product (increase in material consumption).

Motion mode is the most determining factor affecting the stress-strain state of a standard tank. The studied motion modes of the tank, depending on the degree of their influence on the stress-strain state, can be arranged in a row (as σ_{max} decreases): "braking", "acceleration", "jump" and "landing". The "heaviest" mode for a standard tank is "braking". For this mode, the maximum stresses were recorded in the calculations, ranging from 33 to 70.5 MPa (wall thickness – 8 mm and transported fertilizer density – 1,700 kg/m^3. The "acceleration" motion mode causes σ_{max} of no more than 60 % of the maximum stresses characteristic of the "braking" mode. The "lightest" mode for a standard tank is "landing". In the "landing" motion mode of the tank, σ_{max} is no more than 28 % of the maximum stresses characteristic of the "braking" mode. In general, the results of FEM calculations of the elements are consistent with the field tests of standard tanks. During field tests, destruction of a standard tank was observed near the filler neck, in this region FEM calculations showed a local area of maximum stresses.

2. Based on the method of probabilistic deterministic planning, an equation is proposed for calculating maximum stresses depending on LMF density, wall thickness and motion mode of the tank. Nomograms were built that make it possible to quickly determine the wall thickness of a standard tank without calculations, depending on the density of liquid mineral fertilizer and permissible stresses for the plastic used. From the results of FEM calculations, several recommendations can be formulated for adjusting the standard tank design: remove the planes for embedding shut-off valves, change the filler neck design and increase the radius of the tank roof transition to the upper stiffeners.

Conflict of interest

The authors declare that they have no conflict of interest in relation to this research, whether financial, personal, authorship or otherwise, that could affect the research and its results presented in this paper.

Financing

This research is funded by the Science Committee of the Ministry of Science and Higher Education of the Republic of Kazakhstan (Grant No. AP14870434).

Data availability

Manuscript has data included as electronic supplementary material.

Use of artificial intelligence

The authors confirm that they did not use artificial intelligence technologies when creating the current work.

Acknowledgments

During the research, the staff of the Department of "Chemistry and Chemical Technology" of the M. Kozybayev North-Kazakhstan University and the management of

AVAGRO LLP provided significant assistance. This research is funded by the Science Committee of the Ministry of Science and Higher Education of the Republic of Kazakhstan (Grant No. AP14870434).

References

1. Crawford, R. J., Throne, J. L. (2002). Rotational Molding Technology. William Andrew.
2. Gupta, N., Ramkumar, P., Sangani, V. (2020). An approach toward augmenting materials, additives, processability and parameterization in rotational molding: a review. Materials and Manufacturing Processes, 35 (14), 1539–1556. https://doi.org/10.1080/10426914.2020.1779934
3. Crawford, R. J. (1996). Recent advances in the manufacture of plastic products by rotomoulding. Journal of Materials Processing Technology, 56 (1-4), 263–271. https://doi.org/10.1016/0924-0136(95)01840-9
4. Gnanaprakasam, P. D., Vanisree, A. J. (2022). Recurring detrimental impact of agrochemicals on the ecosystem, and a glimpse of organic farming as a possible rescue. Environmental Science and Pollution Research, 29 (50), 75103–75112. https://doi.org/10.1007/s11356-022-22750-1
5. Hossain, M. E., Shahrukh, S., Hossain, S. A. (2022). Chemical Fertilizers and Pesticides: Impacts on Soil Degradation, Groundwater, and Human Health in Bangladesh. Water Science and Technology Library, 63–92. https://doi.org/10.1007/978-3-030-95542-7_4
6. Khan, M. N., Mobin, M., Abbas, Z. K., Alamri, S. A. (2018). Fertilizers and Their Contaminants in Soils, Surface and Groundwater. Encyclopedia of the Anthropocene, 225–240. https://doi.org/10.1016/b978-0-12-809665-9.09888-8
7. Timoshenko, S. (1956). Strength of Material. Part II. Advanced Theory and Problems. Princeton.
8. Klabukova, L. S. (1980). The differential operator of problems of the theory of momentless elastic shells and their solution by the variational-difference method. USSR Computational Mathematics and Mathematical Physics, 20 (1), 225–244. https://doi.org/10.1016/0041-5553(80)90075-0
9. Paimushin, V. N., Shalashilin, V. I. (2006). Geometrically non-linear equations in the theory of momentless shells with applications to problems on the non-classical forms of loss of stability of a cylinder. Journal of Applied Mathematics and Mechanics, 70 (1), 91–101. https://doi.org/10.1016/j.jappmathmech.2006.03.006
10. Zha, S., Lan, H. (2021). Fracture behavior of pre-cracked polyethylene gas pipe under foundation settlement by extended finite element method. International Journal of Pressure Vessels and Piping, 189, 104270. https://doi.org/10.1016/j.ijpvp.2020.104270
11. Khademi-Zahedi, R., Shishesaz, M. (2019). Application of a finite element method to stress distribution in buried patch repaired polyethylene gas pipes. Underground Space, 4 (1), 48–58. https://doi.org/10.1016/j.undsp.2018.05.001
12. Khademi-Zahedi, R. (2019). Application of the finite element method for evaluating the stress distribution in buried damaged polyethylene gas pipes. Underground Space, 4 (1), 59–71. https://doi.org/10.1016/j.undsp.2018.05.002
13. Kochanov, V., Píštěk, V., Kondratiev, A., Yuresko, T., Ku era, P. (2022). Influence of Geometric Parameters of Conical Acrylic Portholes on Their Stress–Strain Behaviour. Polymers, 14 (5), 1041. https://doi.org/10.3390/polym14051041
14. Karamnov E. I. Application of the finite element method to solve the problem of stability of the tank wall. Applied research and development in priority areas of science and technology. Available at: http://econf.rae.ru/article/7560
15. Vijay, K., Jayapalan, S. (2022). Creep analysis of Water tank made of Polypropylene (PP) and High-Density Polyethylene (HDPE) polymer material using ANSYS Simulation. Journal of Engineering Research. https://doi.org/10.36909/jer.17611
16. Edlabadkar, O., Potdar, S., Jha, H. K., Jaiswal, N. G. (2022). Structural analysis of a rotomolded water tank. International Research Journal of En-gineering and Technology (IRJET). Available at: https://issuu.com/irjet/docs/irjet-v9i741#google_vignette
17. Šuba, O., Bílek, O., Kubišová, M., Pata, V., Měřínská, D. (2022). Evaluation of the Flexural Rigidity of Underground Tanks Manufactured by Rotomolding. Applied Sciences, 12 (18), 9276. https://doi.org/10.3390/app12189276
18. Pozhil, S. N., Menon, N. M., Waigaonkar, S. D., Chaudhari, V. (2020). An analytical model to predict the creep behaviour of linear low-density polyethylene (LLDPE) and polypropylene (PP) used in rotational moulding. Materials Today: Proceedings, 28, 888–892. https://doi.org/10.1016/j.matpr.2019.12.318
19. Tyukanko, V., Demyanenko, A., Semenyuk, V., Dyuryagina, A., Alyoshin, D., Tarunin, R., Voropaeva, V. (2023). Development of an Ultrasonic Method for the Quality Control of Polyethylene Tanks Manufactured Using Rotational Molding Technology. Polymers, 15 (10), 2368. https://doi.org/10.3390/polym15102368
20. Dyuryagina, A., Lutsenko, A., Demyanenko, A., Tyukanko, V., Ostrovnoy, K., Yanevich, A. (2022). Modeling the wetting of titanium dioxide and steel substrate in water-borne paint and varnish materials in the presence of surfactants. Eastern-European Journal of Enterprise Technologies, 1 (6 (115)), 31–42. https://doi.org/10.15587/1729-4061.2022.252757
21. Tyukanko, V., Demyanenko, A., Dyuryagina, A., Ostrovnoy, K., Lezhneva, M. (2021). Optimization of the Composition of Silicone Enamel by the Taguchi Method Using Surfactants Obtained from Oil Refining Waste. Polymers, 13 (21), 3619. https://doi.org/10.3390/polym13213619
22. Tyukanko, V., Demyanenko, A., Dyuryagina, A., Ostrovnoy, K., Aubakirova, G. (2022). Optimizing the Composition of Silicone Enamel to Ensure Maximum Aggregative Stability of Its Suspensions Using Surfactant Obtained from Oil Refining Waste. Polymers, 14 (18), 3819. https://doi.org/10.3390/polym14183819
23. Dyuryagina, A. N., Lutsenko, A. A., Tyukanko, V. Yu. (2019). Study of the disperse effect of polymeric surface-active substances in acrylic dispersions used for painting oil well armature. Bull. Tomsk. Polytech. Univ. Geo Assets Eng., 330 (8), 37–44.
24. E-ECE-TRANS-505. Soglasheniya o prinyatii edinoobraznyh tekhnicheskih predpisaniy dlya kolesnyh transportnyh sredstv, predmetov oborudovaniya i chastey, kotorye mogut byt' ustanovleny i/ili ispol'zovany na kolesnyh transportnyh sredstvah, i ob usloviyah vzaimnogo priznaniya ofitsial'nyh utverzhdeniy, vydavaemyh na osnove etih predpisaniy.